



Dissecting the role of leucine zippers in the binding of bZIP domains of Jun transcription factor to DNA

Kenneth L. Seldeen, Caleb B. McDonald, Brian J. Deegan, Vikas Bhat, Amjad Farooq *

Department of Biochemistry & Molecular Biology and USylvester Braman Family Breast Cancer Institute, Leonard Miller School of Medicine, University of Miami, Miami, FL 33136, USA

ARTICLE INFO

Article history:

Received 11 March 2010

Available online 21 March 2010

Keywords:

AP1–DNA thermodynamics

Jun transcription factor

bZIP family

Leucine zippers

Isothermal titration calorimetry

Analytical laser scattering

ABSTRACT

Leucine zippers, structural motifs typically comprised of five successive heptads of amino acids with a signature leucine at every seventh position, play a central role in the dimerization of bZIP family of transcription factors and their subsequent binding to the DNA promoter regions of target genes. Herein, using analytical laser scattering (ALS) in combination with isothermal titration calorimetry (ITC), we study the effect of successive C-terminal truncation of leucine zippers on the dimerization and energetics of binding of bZIP domains of Jun transcription factor to its DNA response element. Our data show that all five heptads are critical for the dimerization of bZIP domains and that the successive C-terminal truncation of residues leading up to each signature leucine significantly compromises the binding of bZIP domains to DNA. Taken together, our study provides novel insights into the energetic contributions of leucine zippers to the binding of bZIP domains of Jun transcription factor to DNA.

© 2010 Elsevier Inc. All rights reserved.

1. Introduction

bZIP family of transcription factors bind to promoter regions of target genes by virtue of their ability to homodimerize or heterodimerize with other bZIP members in a highly selective manner [1]. All members of the bZIP family are evolutionarily related and share a core modular architecture comprised of a basic zipper (bZIP) domain flanked by a trans-activation (TA) domain either at the N-terminus or C-terminus. The bZIP domain can be further dissected into two well-defined functional subdomains termed the basic region (BR) at the N-terminus followed by the leucine zipper (LZ) at the C-terminus. The leucine zipper is a highly conserved protein module and usually contains a signature leucine at every seventh position within the five successive heptads of amino acid residues. The leucine zippers drive the homo- and hetero-association of bZIP members and adapt continuous α -helices in the context of a dimer by virtue of their ability to wrap around each other into a parallel dimeric coiled coil with a slight left-handed twist [2–4]. Such intermolecular arrangement brings the basic regions at the N-termini of bZIP domains into close proximity and thereby enables them to insert into the major grooves of DNA at the promoter regions in an optimal fashion in a manner akin to a pair of forceps [5–7]. Despite their key role, the effect of successive C-terminal truncation of leucine zippers on the dimerization and energetics of binding of bZIP domains to DNA has hitherto not been assessed. In an effort to address this issue, we undertook studies on the dimerization and the

binding of wildtype and various C-terminal truncated constructs of bZIP domains of Jun—a member of the AP1 (activator protein 1) family of transcription factors involved in executing the terminal stage of many critical signaling cascades that initiate at the cell surface and reach their climax in the nucleus [8,9]—to the TPA (12-O-tetradecanoylphorbol-13-acetate) response element (TRE) containing the TGACTCA consensus motif. Using analytical laser scattering (ALS) in combination with isothermal titration calorimetry (ITC), our data show that all five heptads within leucine zippers are critical for the dimerization of bZIP domains and that the successive C-terminal truncation of residues leading up to each signature leucine significantly compromises the binding of bZIP domains to DNA.

2. Materials and methods

2.1. Protein preparation

Wildtype (WT) and various truncated constructs (Δ L5, Δ L54, Δ L543, Δ L5432 and Δ L54321) of bZIP domain of human Jun, as illustrated in Fig. 1, were cloned into pET102 bacterial expression vector, with an N-terminal thioredoxin (Trx)-tag and a C-terminal polyhistidine (His)-tag, using Invitrogen TOPO technology. Note that each truncated construct contains successive truncation of residues up to and including the signature leucine from the C-terminus of bZIP domain. Thus, the Δ L5 construct is comprised of all residues within the bZIP domain but the C-terminal residues up to and including L5, the Δ L54 construct is comprised of all residues within the bZIP domain but the C-terminal residues up to and

* Corresponding author. Fax: +1 305 243 3955.

E-mail address: amjad@farooqlab.net (A. Farooq).



Fig. 1. A schematic showing the organization and boundaries of wildtype (WT) and various truncated constructs ($\Delta L5$, $\Delta L54$, $\Delta L543$, $\Delta L5432$ and $\Delta L54321$) of bZIP domain of human Jun. Amino acid sequence of wildtype bZIP domain of Jun is shown on top and the subdomains encompassing the N-terminal basic region (BR) and the C-terminal leucine zipper (LZ) are colored blue and brown, respectively. The five signature leucines, designated herein L1–L5, characteristic of LZ subdomains are boxed and bold faced. (For interpretation of the references to color in this figure legend, the reader is referred to the web version of this article.)

including L4, and so on. Recombinant proteins were subsequently expressed in *Escherichia coli* Rosetta2 (DE3) bacterial strain (Novagen) and purified on a Ni–NTA affinity column using standard procedures. Treatment on a Hiload Superdex 200 size-exclusion chromatography column coupled to GE Akta FPLC system led to purification of recombinant proteins to apparent homogeneity as judged by SDS–PAGE analysis. Further characterization of recombinant proteins was conducted as described previously [10].

2.2. DNA synthesis

15-mer DNA oligos containing the TRE consensus site TGACTCA were commercially obtained from Sigma Genosys. The complete nucleotide sequences of the sense and antisense oligos constituting the TRE duplex is presented below:

5'-cgcgTGACTCAccc-3'
3'-gcgcACTGAGTggg-5'

Oligo concentrations were determined spectrophotometrically and annealed together to form TRE duplexes as described earlier [11].

2.3. ALS experiments

Analytical laser scattering (ALS) experiments were conducted on a Wyatt miniDAWN TREOS triple-angle static laser light scattering detector coupled in-line with a Wyatt Optilab rEX refractive index detector and interfaced to a Hiload Superdex 200 size-exclusion chromatography column under the control of a GE Akta FPLC system within a chromatography refrigerator at 4 °C. Wildtype (WT) and various truncated constructs ($\Delta L5$, $\Delta L54$, $\Delta L543$, $\Delta L5432$ and $\Delta L54321$) of bZIP domain of human Jun were loaded onto the column at a flow rate of 1 ml/min and the data were automatically acquired using the ASTRA software. All protein samples were prepared in 50 mM Tris, 200 mM NaCl, 5 mM β -mercaptoethanol and 1 mM EDTA at pH 8.0 and the starting concentrations injected onto the column were between 20 and 50 μ M. The angular- and concentration-dependence of Rayleigh scattering intensity of each protein construct was fit to the built-in Zimm equation [12,13]:

$$(Kc/R_\theta) = ((1/M) + 2A_2c) \left[1 + \left((16\pi^2 r^2 / 3\lambda^2) \sin^2(\theta/2) \right) \right] \quad (1)$$

where R_θ is the excess Rayleigh ratio due to protein in the solution as a function of protein concentration c (mg/ml) and the scattering angle θ (42°, 90° and 138°), M is the molecular mass of protein, A_2 is the second virial coefficient, λ is the wavelength of laser light in solution (658 nm), r is the radius of gyration of protein and K is given by the following relationship:

$$K = [4\pi^2 n^2 (dn/dc)^2] / N_A \lambda^4 \quad (2)$$

where n is the refractive index of the solvent, dn/dc is the refractive index increment of the protein in solution, N_A is the Avogadro's number (6.02×10^{23} /mol), λ is the wavelength of laser light in solution (658 nm) and c is the protein concentration. If we assume that $c \rightarrow 0$ and $\theta \rightarrow 0$, then Eq. (1) reduces to:

$$(Kc/R_\theta) = 1/M \quad (3)$$

Thus, under conditions, where $c \rightarrow 0$ and $\theta \rightarrow 0$, the y-intercept (b) of Eq. (1) is given by:

$$b = 1/M \Rightarrow M = 1/b \quad (4)$$

Accordingly, the weighted average value for the molecular mass (M) of each protein construct was obtained from the y-intercept of linear fits of a range of $(Kc/R_\theta) - \sin^2(\theta/2)$ plots for a total of ~ 500 data slices in the limit of low protein concentrations along the elution profile at three scattering angles.

2.4. ITC measurements

Isothermal titration calorimetry (ITC) experiments were performed on a Microcal VP-ITC instrument and data were acquired and processed using Microcal ORIGIN software. All measurements were repeated 2–3 times. Briefly, wildtype (WT) and various truncated constructs ($\Delta L5$, $\Delta L54$, $\Delta L543$, $\Delta L5432$ and $\Delta L54321$) of bZIP domain of Jun and TRE duplex were prepared in 50 mM Tris, 200 mM NaCl, 1 mM EDTA and 5 mM β -mercaptoethanol at pH 8.0. The experiments were initiated by injecting $25 \times 10 \mu$ l aliquots of 100–500 μ M of TRE duplex from the syringe into the calorimetric cell containing 1.8 ml of 5–50 μ M of a bZIP construct at 25 °C. To extract observed affinity (K_d) and observed enthalpy

(ΔH), the binding isotherms were iteratively fit to the following built-in function by non-linear least squares regression analysis using the integrated Microcal ORIGIN software:

$$q(i) = (nVP\Delta H/2)\{[1 + (L/nP) + (K_d/nP)] - [[1 + (L/nP) + (K/nP)]^2 - (4L/nP)]^{1/2}\} \quad (5)$$

where $q(i)$ is the heat release (kcal mol^{-1}) for the i th injection, n is the binding stoichiometry, V is the effective volume of protein solution in the calorimetric cell (1.46 ml), P is the total dimer-equivalent concentration of a bZIP construct in the calorimetric cell (μM) and L is the concentration of TRE duplex added (μM). The above equation is derived from the binding of a ligand to a macromolecule using the law of mass action assuming one-site model [14]. Observed free energy of binding (ΔG) was calculated from the relationship:

$$\Delta G = RT \ln K_d \quad (6)$$

where R is the universal molar gas constant (1.99 cal/mol/K) and T is the absolute temperature (298 K). Observed entropic contribution ($T\Delta S$) to binding was calculated from the relationship:

$$T\Delta S = \Delta H - \Delta G \quad (7)$$

All other control experiments were conducted as described previously [10,11].

3. Results and discussion

3.1. Integrity of all five heptads within the leucine zippers is critical for the dimerization of bZIP domains

The leucine zippers, comprised of a signature leucine at every seventh position within the five successive heptads of amino acid residues, promote the dimerization of bZIP domains [1]. In an effort to determine how the successive C-terminal truncation of leucine zippers affects their ability to dimerize, we analyzed the oligomericity of wildtype (WT) and various truncated constructs ($\Delta L5$, $\Delta L54$, $\Delta L543$, $\Delta L5432$ and $\Delta L54321$) of bZIP domain of Jun using ALS—an absolute method for characterizing hydrodynamic properties of macromolecules in solution. Fig. 2 shows elution profiles as monitored by changes in the refractive index of each bZIP con-

struct in solution on the Superdex 200 size-exclusion chromatography column and corresponding partial Zimm plots for each bZIP construct. It is clearly evident from these data that the elution profiles of WT, $\Delta L54$, $\Delta L543$, $\Delta L5432$ and $\Delta L54321$ constructs contain single peaks, implying that these constructs are comprised of only one species. In contrast, the elution profile of $\Delta L5$ construct is comprised of a sharp peak with a shoulder, implying that it consists of more than one species. Table 1 provides the molecular masses of the various bZIP constructs as determined from Zimm analysis corresponding to each peak. It is notable that while the $\Delta L54$, $\Delta L543$, $\Delta L5432$ and $\Delta L54321$ constructs are monomeric in solution, the WT construct is dimeric. Additionally, the two peaks observed in the elution profile of $\Delta L5$ construct correspond to monomeric and dimeric species, implying that this construct most likely exists in dimer–monomer equilibrium with the latter species being dominant in solution. Collectively, our data indicate that the integrity of all five heptads within the leucine zippers is critical for the dimerization of bZIP domains of Jun and that even the slight truncation of residues up to and including the C-terminal signature leucine, L5, significantly compromises their dimerization. It should however be borne in mind that residues intervening the five signature leucines, L1–L5, also play a key role in the dimerization and specificity of leucine zippers and thus their dimerization potential is also likely to be dictated by the nature of amino acid sequence in addition to the number of residues.

3.2. Successive C-terminal truncation of leucine zippers significantly compromises the binding of bZIP domains to DNA

The dimerization of leucine zippers brings the basic regions at the N-termini of bZIP domains into close proximity and thereby enables them to insert into the major grooves of DNA at the promoter regions in an optimal fashion in a manner akin to a pair of forceps [5–7]. In an attempt to understand how successive C-terminal truncation of leucine zippers affects the energetics of binding of bZIP domains to DNA, we conducted ITC analysis. It is of worthy note that ITC offers a direct and continuous method for studying underlying thermodynamics associated with protein–ligand interactions. Fig. 3 shows representative ITC isotherms for the binding of TRE duplex to wildtype (WT) and various truncated constructs ($\Delta L5$, $\Delta L54$, $\Delta L543$, $\Delta L5432$ and $\Delta L54321$) of bZIP

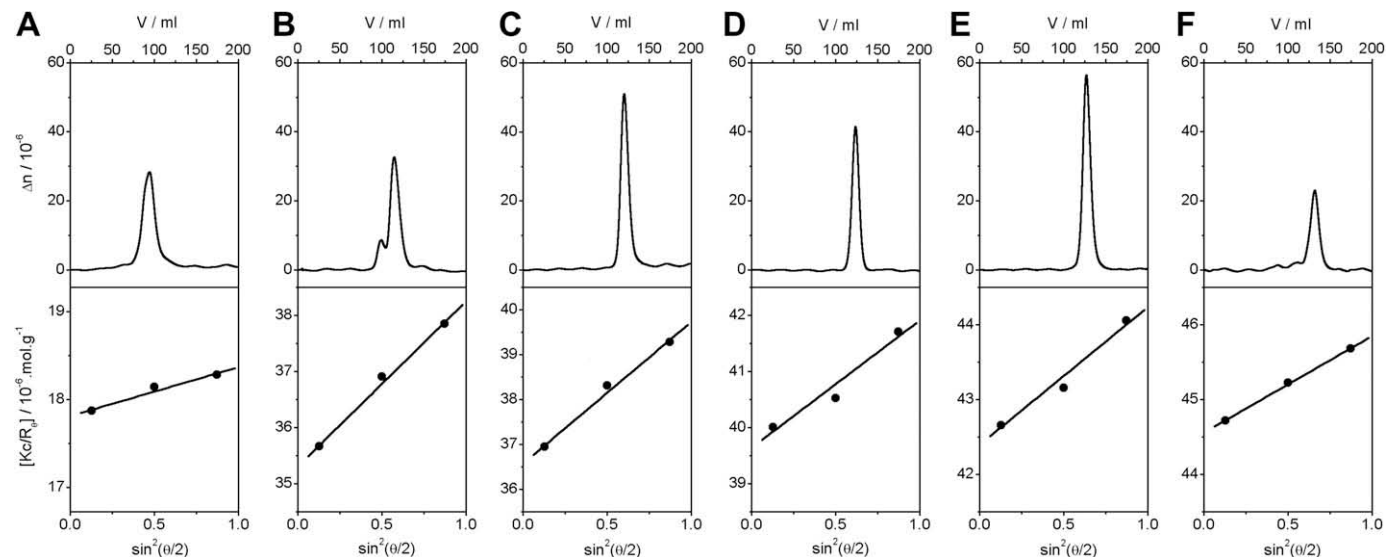


Fig. 2. Representative ALS profiles for WT (A), $\Delta L5$ (B), $\Delta L54$ (C), $\Delta L543$ (D), $\Delta L5432$ (E) and $\Delta L54321$ (F) constructs of bZIP domain of Jun. The upper panels show elution profiles with differential refractive index (Δn) of each construct plotted as a function of elution volume (V). Note that Δn is a dimensionless parameter expressed here in absolute terms. In the lower panels, partial Zimm plots of various constructs at maximal protein concentrations along the corresponding elution profiles are shown. The solid lines through the data points in the lower panels represent linear fits.

Table 1

Calculated molecular mass (M_{cal}) and observed molecular mass (M_{obs}) for the wildtype (WT) and various truncated constructs of bZIP domain of Jun.

	M_{cal} (kDa)	M_{obs} (kDa)	Oligomericity
WT	25.2	52.2 ± 3.0	Dimer
ΔL5	24.5	48.2 ± 4.0	Dimer
ΔL54	23.5	26.3 ± 0.7	Monomer
ΔL543	22.8	24.9 ± 2.3	Monomer
ΔL5432	22.2	23.8 ± 0.9	Monomer
ΔL54321	21.2	22.8 ± 0.7	Monomer
ΔL54321	21.2	21.6 ± 1.6	Monomer

M_{cal} was calculated from the amino acid sequence of each bZIP construct including all residues within the N-terminal Trx-tag and the C-terminal His-tag. M_{obs} for each bZIP construct was obtained from ALS analysis. Errors were calculated from 2 to 3 independent measurements. All errors are given to one standard deviation.

domain of Jun. Complete thermodynamic profiles for these protein–DNA interactions are provided in Table 2. Our data suggest that while the WT, ΔL5, ΔL54, ΔL543 constructs of bZIP domain bind to DNA, no binding is observed for the ΔL5432 and ΔL54321 constructs. Increasing the protein concentration in the calorimetric cell or DNA concentration in the syringe and/or varying the temperature of ITC experiments had no effect on these observations, implying that the ΔL5432 and ΔL54321 constructs indeed lack intrinsic affinity for DNA in lieu of lack of any observable change in the heat of binding. Although integrity of all five heptads within leucine zippers is not critical for the binding of bZIP domains to DNA with physiologically-relevant affinities, it is notable that successive C-terminal truncation substantially compro-

mises their binding energetics (Table 2). Thus, the ΔL5, ΔL54 and ΔL543 constructs bind to TRE duplex with affinities that are between 5- and 60-fold weaker relative to the WT construct. It should also be noted that despite their highly compromised energetics, the ΔL5, ΔL54 and ΔL543 constructs bind to TRE duplex with stoichiometries of 1:1 in a manner akin to the binding of WT construct. Given that the ΔL5, ΔL54 and ΔL543 constructs are largely monomeric in solution (Fig. 2 and Table 1), it is not clear whether they become dimerized upon binding to TRE duplex or whether they bind to each half-site within the TRE duplex in an independent manner.

3.3. Binding of wildtype and various truncated bZIP constructs to DNA is enthalpy–entropy compensated

Enthalpy–entropy compensation is a phenomenon that is widely observed in biological systems [15]. In a nutshell, it postulates that enthalpic contributions to macromolecular interactions are compensated by equal but opposing entropic changes such that there is no net gain in the overall free energy. Fig. 4a shows the enthalpy–entropy compensation plot for the binding of TRE duplex to wildtype (WT) and various truncated constructs (ΔL5, ΔL54, ΔL543) of bZIP domain of Jun. Evidently, the binding of various constructs of bZIP domain to TRE duplex exquisitely obeys the phenomenon of enthalpy–entropy compensation. It should be noted however that the enthalpy–entropy compensation is not an absolute thermodynamic law nor it ought to be obeyed universally. Indeed, if it were to be obeyed, macromolecular interactions would

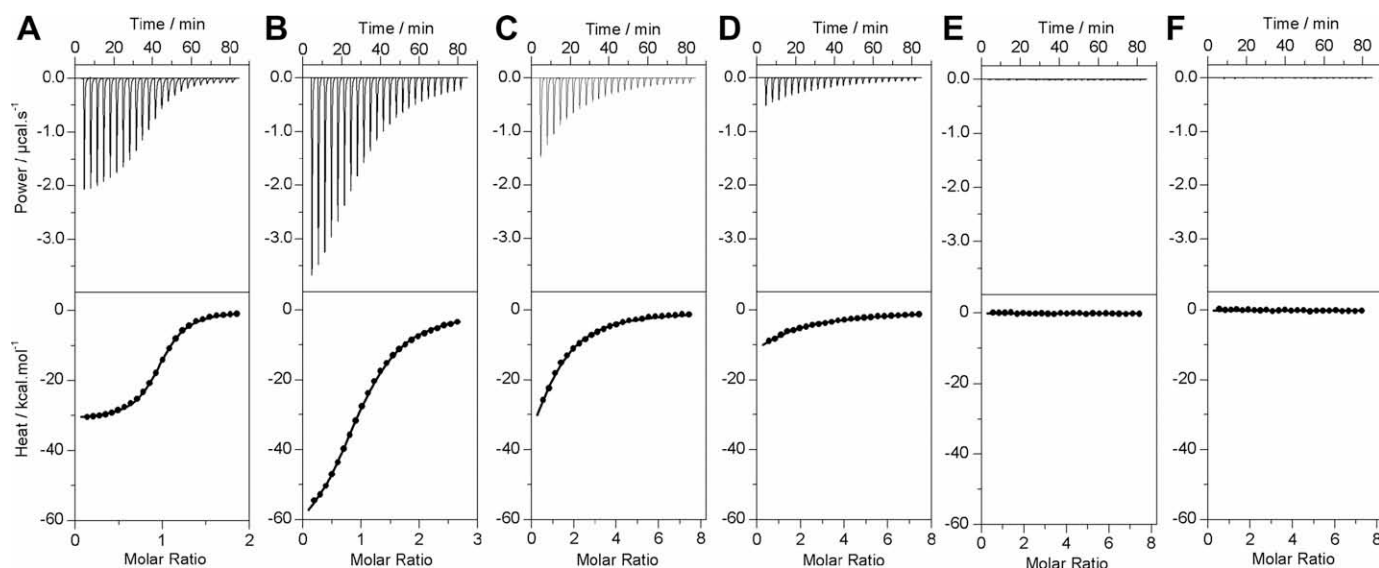


Fig. 3. Representative ITC isotherms for the binding of TRE duplex to WT (A), ΔL5 (B), ΔL54 (C), ΔL543 (D), ΔL5432 (E) and ΔL54321 (F) constructs of bZIP domain of Jun. The upper panels show the raw ITC data expressed as change in thermal power with respect to time over the period of titration. In the lower panels, change in molar heat is expressed as a function of molar ratio of TRE duplex to dimer-equivalent of each bZIP construct. The solid lines in the lower panels represent the fit of data points to Eq. (5). All data are shown to same scale for direct comparison.

Table 2

Observed thermodynamic parameters for the binding of TRE duplex to wildtype (WT) and various truncated constructs of bZIP domain of Jun.

	n	K_d (μM)	ΔH (kcal mol^{-1})	$T\Delta S$ (kcal mol^{-1})	ΔG (kcal mol^{-1})
WT	0.97 ± 0.01	0.25 ± 0.01	−31.22 ± 0.05	−22.14 ± 0.09	−9.01 ± 0.02
ΔL5	0.99 ± 0.02	1.26 ± 0.21	−70.75 ± 1.43	−62.58 ± 1.26	−8.06 ± 0.10
ΔL54	1.03 ± 0.02	6.14 ± 0.27	−70.64 ± 0.87	−63.47 ± 0.84	−7.12 ± 0.03
ΔL543	0.97 ± 0.01	14.77 ± 1.67	−46.34 ± 0.88	−39.63 ± 0.84	−6.60 ± 0.07
ΔL5432	NB	NB	NB	NB	NB
ΔL54321	NB	NB	NB	NB	NB

All thermodynamic parameters were calculated from ITC analysis. Errors were calculated from 2 to 3 independent measurements. All errors are given to one standard deviation. Note that no binding (NB) of TRE duplex to ΔL5432 and ΔL54321 constructs was observed.

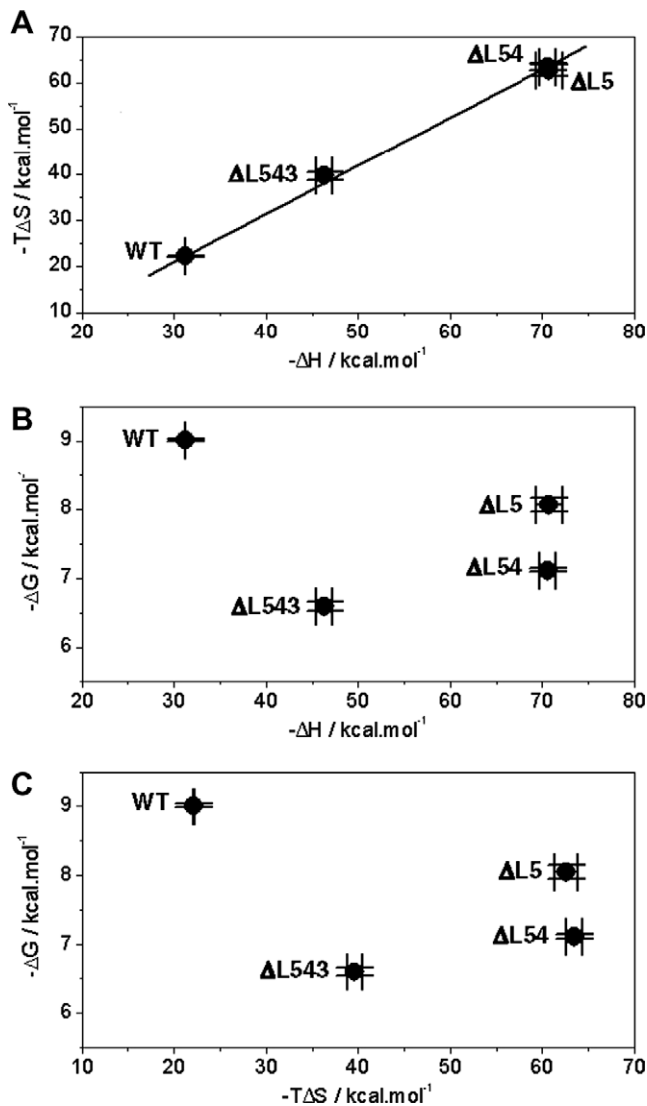


Fig. 4. Inter-dependence of enthalpic change (ΔH), entropic change ($T\Delta S$) and free energy change (ΔG) for the binding of TRE duplex to wildtype (WT) and various truncated constructs ($\Delta L5$, $\Delta L54$ and $\Delta L543$) of bZIP domain of Jun. (A) ΔH - $T\Delta S$ plot. The solid line represents linear fit to the data points. (B) ΔH - ΔG plot. (C) $T\Delta S$ - ΔG plot. Error bars were calculated from 2 to 3 independent measurements. All errors are given to one standard deviation.

be expected to be of similar affinity across the board in lieu of ranging from weak interactions in the micromolar range to ultra-tight interactions in the picomolar range observed in diverse cellular processes. The fact that the binding of various constructs of bZIP domain to DNA is enthalpy-entropy compensated suggests that efforts to design high-affinity synthetic bZIP domains capable of competing with endogenous bZIP domains in the context of therapeutic intervention may go unrewarded unless thermodynamic factors are taken into consideration. Importantly, further studies are warranted to unlock the thermodynamic basis of enthalpy-entropy compensation observed here in the case of binding of various bZIP constructs to DNA.

3.4. Enthalpic and entropic contributions do not correlate with the binding energy of wildtype and various truncated bZIP constructs to DNA

Given that protein-DNA interactions at the major groove are largely governed by the formation of intermolecular salt bridges and an

extensive network of hydrogen bonding, it comes as no surprise that the binding of proteins to the DNA major groove is largely driven by enthalpy accompanied by entropic penalty [16]. In light of this salient observation, we next asked the question whether there was any correlation between enthalpy and entropy versus the overall free energy for the binding of TRE duplex to wildtype (WT) and various truncated constructs ($\Delta L5$, $\Delta L54$, $\Delta L543$) of bZIP domain of Jun. As is clearly evident from the plots shown in Fig. 4b and c, our data show that an increase in free energy neither correlates with favorable enthalpy nor favorable entropy in agreement with the enthalpy-entropy compensation phenomenon discussed above. In other words, a small favorable enthalpy may be sufficient to generate a high binding affinity by virtue of a small corresponding entropic penalty. Conversely, a large favorable enthalpy does not necessarily result in tighter binding due to a compensating increase in entropic penalty. Indeed, close scrutiny of various thermodynamic parameters reported in Table 2, reveals that while the binding of $\Delta L5$, $\Delta L54$ and $\Delta L543$ constructs to TRE duplex is 5- to 60-fold weaker relative to the WT construct, the enthalpic contribution to the overall free energy for these constructs is much larger than that observed for the WT construct. However, the binding of $\Delta L5$, $\Delta L54$ and $\Delta L543$ constructs to TRE duplex also suffers from an equally larger unfavorable entropic contribution and thereby compensates any enthalpic gain to the overall free energy. What might be the basis of rather large enthalpic contribution to the overall free energy for the binding of $\Delta L5$, $\Delta L54$ and $\Delta L543$ constructs to TRE duplex relative to the WT construct? Several lines of evidence suggest that leucine zippers are unstable as α -helices when in isolation and only fold into α -helices in the context of a coiled coil dimer [17–19]. This is believed to be due to the fact that the dimer interface of a coiled coil is comprised of hydrophobic residues, created largely by the interdigitation of signature leucines from each α -helix, and thus an isolated α -helical leucine zipper is thermodynamically unstable in isolation. It is also worthy note that the basic regions within the bZIP domains are unstructured in the absence of DNA and undergo folding to adapt α -helical conformations only upon DNA binding [20]. In light of these observations coupled with the fact that the $\Delta L5$, $\Delta L54$ and $\Delta L543$ constructs are largely monomeric in solution (Fig. 2 and Table 1), the most straightforward interpretation for the rather large enthalpic contribution to the overall free energy for the binding of $\Delta L5$, $\Delta L54$ and $\Delta L543$ constructs to TRE duplex relative to the WT construct is that they dimerize upon binding to DNA in a coupled folding-binding manner. In other words, the thermodynamic parameters reported in Table 2 represent composite contributions from the folding and subsequent binding of various constructs of bZIP domains to DNA. Accordingly, it also follows that DNA is capable of inducing dimerization of leucine zippers, implying that DNA may also exercise an important role in determining the dimerization and specificity of bZIP members.

4. Conclusions

Leucine zippers play a central role in the physiological action of bZIP family of transcription factors by virtue of their ability to promote homodimerization of a particular bZIP member or heterodimerization between distinct members of bZIP family. The ability of leucine zippers of two distinct members to come together into a dimeric coiled coil thus underlies the basis of their specificity and diversity for the recognition of a wide spectrum of promoter elements with high selectivity. For example, human bZIP family is comprised of ~50 distinct members, implying that there are potentially over 2000 distinct bZIP dimers primed for the recognition of as many unique promoter elements with high fidelity. Given the importance of leucine zippers to the specificity and diversity of bZIP transcription factors, our present study set out

to evaluate the effect of successive C-terminal truncation of leucine zippers on the dimerization and energetics of binding of bZIP domains of Jun transcription factor to its DNA response element. Our data clearly suggest that the integrity of all five heptads within leucine zippers is critical for their dimerization and that successive C-terminal truncations severely compromise the energetics of binding of bZIP domains to DNA. Furthermore, our study also provokes a key role of DNA in the dimerization and specificity of bZIP members and argues strongly that the design of future drugs harboring greater efficacy coupled with low toxicity could benefit from the consideration of underlying thermodynamic forces. Taken together, our data offer new insights into the significance of leucine zippers in the physiological action of bZIP transcription factors and advance our understanding of the thermodynamic forces that dictate their functional diversity and specificity.

Acknowledgments

This work was supported by funds from the National Institutes of Health (Grant# R01-GM083897) and the USylvester Braman Family Breast Cancer Institute to A.F. C.B.M. is a recipient of a postdoctoral fellowship from the National Institutes of Health (Award# T32-CA119929). B.J.D. and A.F. are members of the Sheila and David Fuente Graduate Program in Cancer Biology at the Sylvester Comprehensive Cancer Center of the University of Miami.

References

- [1] K.A. Lee, Dimeric transcription factor families: it takes two to tango but who decides on partners and the venue?, *J Cell Sci.* 103 (Pt. 1) (1992) 9–14.
- [2] E.K. O'Shea, R. Rutkowski, W.F. Stafford 3rd, P.S. Kim, Preferential heterodimer formation by isolated leucine zippers from fos and jun, *Science* 245 (1989) 646–648.
- [3] E.K. O'Shea, R. Rutkowski, P.S. Kim, Evidence that the leucine zipper is a coiled coil, *Science* 243 (1989) 538–542.
- [4] E.K. O'Shea, R. Rutkowski, P.S. Kim, Mechanism of specificity in the Fos–Jun oncoprotein heterodimer, *Cell* 68 (1992) 699–708.
- [5] E.K. O'Shea, J.D. Klemm, P.S. Kim, T. Alber, X-ray structure of the GCN4 leucine zipper, a two-stranded, parallel coiled coil, *Science* 254 (1991) 539–544.
- [6] P. Konig, T.J. Richmond, The X-ray structure of the GCN4-bZIP bound to ATF/CREB site DNA shows the complex depends on DNA flexibility, *J. Mol. Biol.* 233 (1993) 139–154.
- [7] J.N. Glover, S.C. Harrison, Crystal structure of the heterodimeric bZIP transcription factor c-Fos–c-Jun bound to DNA, *Nature* 373 (1995) 257–261.
- [8] P. Angel, M. Karin, The role of Jun, Fos and the AP-1 complex in cell-proliferation and transformation, *Biochim. Biophys. Acta* 1072 (1991) 129–157.
- [9] Y. Chinenov, T.K. Kerppola, Close encounters of many kinds: Fos–Jun interactions that mediate transcription regulatory specificity, *Oncogene* 20 (2001) 2438–2452.
- [10] K.L. Seldeen, C.B. McDonald, B.J. Deegan, A. Farooq, Coupling of folding and DNA-binding in the bZIP domains of Jun–Fos heterodimeric transcription factor, *Arch. Biochem. Biophys.* 473 (2008) 48–60.
- [11] K.L. Seldeen, C.B. McDonald, B.J. Deegan, A. Farooq, Single nucleotide variants of the TGAACA motif modulate energetics and orientation of binding of the Jun–Fos heterodimeric transcription factor, *Biochemistry* 48 (2009) 1975–1983.
- [12] B.H. Zimm, The scattering of light and the radial distribution function of high polymer solutions, *J. Chem. Phys.* 16 (1948) 1093–1099.
- [13] P.J. Wyatt, Light scattering and the absolute characterization of macromolecules, *Anal. Chim. Acta* 272 (1993) 1–40.
- [14] T. Wiseman, S. Williston, J.F. Brandts, L.N. Lin, Rapid measurement of binding constants and heats of binding using a new titration calorimeter, *Anal. Biochem.* 179 (1989) 131–137.
- [15] E.B. Starikov, B. Norden, Enthalpy–entropy compensation: a phantom or something useful?, *J Phys. Chem. B* 111 (2007) 14431–14435.
- [16] P.L. Privalov, A.I. Dragan, C. Crane-Robinson, K.J. Breslauer, D.P. Remeta, C.A. Minetti, What drives proteins into the major or minor grooves of DNA?, *J Mol. Biol.* 365 (2007) 1–9.
- [17] M.A. Weiss, Thermal unfolding studies of a leucine zipper domain and its specific DNA complex: implications for scissor's grip recognition, *Biochemistry* 29 (1990) 8020–8024.
- [18] K.S. Thompson, C.R. Vinson, E. Freire, Thermodynamic characterization of the structural stability of the coiled-coil region of the bZIP transcription factor GCN4, *Biochemistry* 32 (1993) 5491–5496.
- [19] H. Qian, A thermodynamic model for the helix–coil transition coupled to dimerization of short coiled-coil peptides, *Biophys. J.* 67 (1994) 349–355.
- [20] L. Patel, C. Abate, T. Curran, Altered protein conformation on DNA binding by Fos and Jun, *Nature* 347 (1990) 572–575.